GAMMA-RAY INDUCED DISPLACEMENT IN D2O REACTORS (u)

N. P. Baumann

Westinghouse Savannah River Company
Savannah River Laboratory
Aiken, South Carolina, USA

ABSTRACT

Gamma-ray damage to tank walls is typically more severe in D2O than in H2O moderated lattices because of the much higher ratios of slow-to-fast neutron flux. To estimate this effect it was first necessary to develop energy dependent gamma-ray displacement cross sections for iron. These, along with coupled neutron-gamma-ray transport computations, provided a measure of displacement damage from this source in SRS reactor tank walls. Gamma-ray displacements originating from high energy gammas from neutron capture in and near the tank wall exceeded those from gamma rays created in the reactor core. The displacements from the combined gamma sources ranged from 13% to 16% of that due to iron atom recoil following neutron capture.

INTRODUCTION

Irradiation of metals by neutrons, gamma rays, or charged particles generally results in damage such as embrittlement and swelling. The damage is due to displacement of metal atoms. To equate damage from the various mechanisms, it is necessary to have a common scale. The concept of Displacements Per Atom (DPA) has been developed, in part, for this purpose (c.f., M. T. Robinson [1]).

High energy gamma rays cause damage in metals from the electrons set in motion by Compton scattering and pair-formation interactions. In light-water power reactors damage from high energy neutrons dominates, primarily because of the high ratio of fast-to-slow neutron flux at the pressure vessel wall. In heavy water reactors, however, this ratio may be reversed and it may be necessary to include the effect of gamma rays along with thermal neutron (n,γ) reactions.

The concept of a "displacement cross section" has been developed for various neutron interactions [2]. The displacement cross section for a material is simply the product of a conventional neutron reaction cross section times the average number of displacements per reaction, summed over all relevant reactions. This paper develops a similar cross section for gamma-ray interaction with iron and applies it to SRS (Savannah River Site) reactor tank-wall conditions.

DISCUSSION

A recent article by Gold, Roberts, and Doran [3] treats the subject of gamma-ray damage. In this paper, the cross section is evaluated in terms of initial beta energy in order to apply it to data from a solid-state detector. For our application, the starting point is a computed gamma-ray spectrum. It was thus necessary to repeat and extend Gold et al., results to obtain the desired gamma-ray displacement cross sections. Their analysis procedure is followed in the present paper except that cross sections are evaluated for one orbital iron electron rather than for one iron atom. A factor of 26 relates the two cross sections for iron. For common stainless steels the average per atom displacement cross section is closely proportional to the average number of orbital electrons. The following steps were employed.

1. Compute the differential rate of energy loss, dE/dX, as a function of electron energy for electrons in iron.

2. Obtain the total number of iron atom displacements as a function of initial electron energy by taking tabulated differential displacement cross sections for electrons and integrating over the distribution of step 1.

3. Compute the energy distribution of scattered electrons and the total cross section for Compton events as a function of gamma-ray energy.

4. Compute the energy distribution of electrons and positrons and the total cross section for pair formation as a function of gamma-ray energy.

5. Compute the number of displacements per Compton event as a function of gamma-ray energy by convoluting steps 2 and 3.

6. Compute the number of displacements per pair formed as a function of gamma-ray energy by convoluting steps 2 and 4.

7. Obtain the displacement cross section per electron (of the iron) as a function of gamma-ray energy by multiplying the results of step 5 by the total Compton cross section of step 3 and summing this with the corresponding product (steps 6 and 4) for pair formation.

(Step 1) Stopping Power for Electrons and Positrons in Iron

A recent compilation of stopping powers for electrons and positrons is given by Seltzer and Berger [4]. These are given in terms of energy dependent coefficients which can be manipulated to derive conventional dE/dX values.

(Step 2) Atom Displacements in Iron by Electrons

The concept of "effective displacement threshold energy" is used in estimating damage due to atom displacements. A value of 40 eV as the threshold energy for iron and stainless steels is now generally used. A threshold of 28 eV was also included to illustrate sensitivity to this parameter.

Differential displacement cross sections, sigma(E), for electrons have been evaluated be Oen [5] for a broad range of elements and threshold energies. The energy grid given by Oen is quite irregular so that graphical interpolation was necessary to perform the numerical integration of the expression:

$$n(E_b) = \int N_a \mathrm{Sigma}(E) dE/(-dE/dX) \qquad (1)$$

where $n(E_b)$ is the total number of iron displacements for an electron of initial energy E_b, N_a is the density (atoms/cm^3)of iron. Sigma (E) is Oen's displacement cross section, and (dE/dX) is the stopping power.

The results are plotted in Figure 1 for 40 eV and 28 eV thresholds. They are shown both for primary displacements from direct electron interaction and including secondary displacements from the motion of the displaced iron atom.

(Steps 3 and 5) Displacements per Compton Electron

Compton scattering is well understood and is discussed in many standard text books (c.f., [6]). The equation for the differential cross section is a straightforward algebraic equation with the energy of the scattered electron as the variable. If this differential cross section is divided by the integrated total cross section one obtains the conditional probability function

$$P_c(E_g,E_b) = \mathrm{Sigma}(E_g,E_b)/\mathrm{Sigma(total)} \qquad (2)$$

where P_c(Eg,Eb) is the probability that if a gamma ray with initial energy E_g undergoes Compton scattering the scattered electron will have energy E_b.

The average number of displacements, $N_c(E_g)$, per Compton event with an initial gamma-ray energy E_g is then given by the integral of the products of equations 1 and 2.

$$N_c(E_g) = \int P_c(E_g,E_b)n(E_b)dE_b \qquad (3)$$

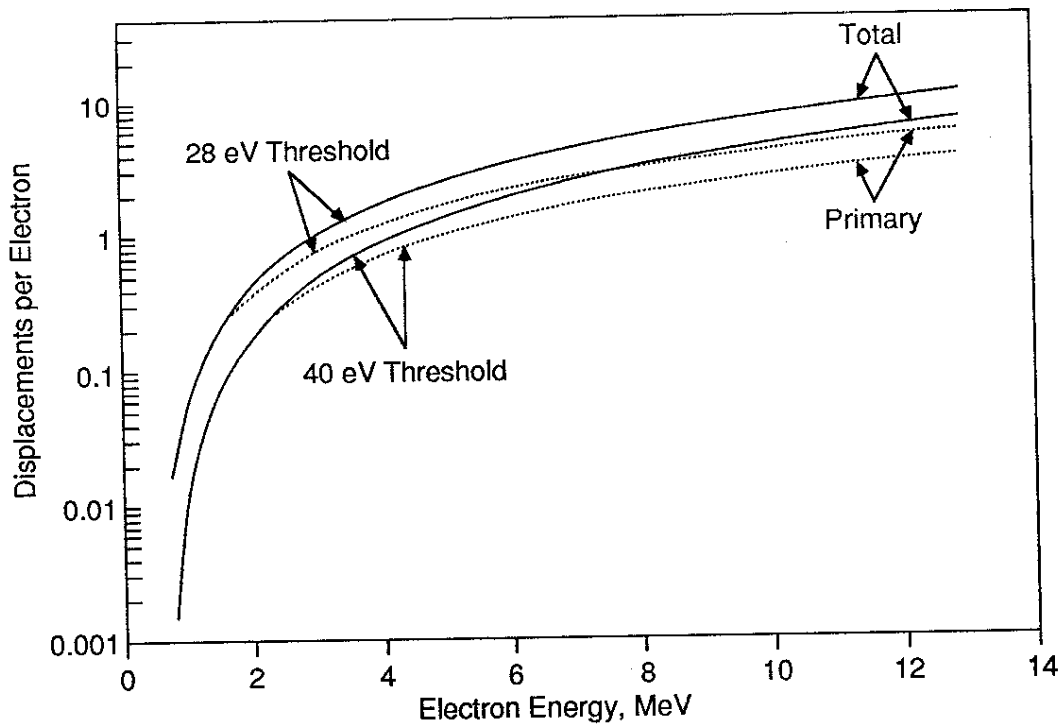

Figure 1. Electron-Induced Displacements in Iron

M91feb028.01
02-21-91

(Steps 4 and 6) Displacements per Pair Formed

In contrast to Compton scattering, pair formation is strongly dependent on the nucleus with which the electron is associated. Except for the energy of 1.022 MeV required to form the pair, the entire energy of the gamma ray goes into kinetic energy of the electron and positron. This energy is not equally divided, but covers the entire range of partition. A rigorous theoretical treatment has not been developed for pair formation, but approximate formulae are given by Hough [7] which just cover the region of interest here. A probability function can be defined as for Compton events as

$$P_p(E_g,E_{fract}) = Sigma(E_g,E_{fract})/Sigma(total) \qquad (4)$$

where E_{fract} is the fraction of total kinetic energy taken up by the positron and the total sigmas are obtained by numerical integration over the allowed range of positron energies, or more accurately by a separate formula given by Hough [7]. The average number of displacements, $N_p(E_g)$, per pair-formation event with gamma energy E_g, is obtained by the integration of the product of equations 1 and 4.

$$N_p(E_g) = \int 2P_p(E_g,E_{fract})n(E_b)dE_b \qquad (5)$$

Here the integration is carried out from zero to the gamma-ray energy minus 1.022 MeV. The factor of two accounts for both electron and positron. No distinction is made for the small difference in the two stopping powers. The results are included in Table I.

Table I
Gamma-ray Interaction Cross Sections on Iron

Eg, MeV	Reaction Xsection*		Displacements per Event**		Total Displacement Xsection*
	Pair	Compton	Pair	Compton	
0.5	0.0	289.3	0.0000	0.0000	0.0
1.0	0.0	211.3	0.0000	0.0010	0.2
1.5	1.1	171.6	0.0000	0.0171	2.9
2.0	4.6	146.4	0.0039	0.0568	8.3
2.5	8.8	128.6	0.0320	0.1203	15.8
3.0	13.1	115.1	0.0900	0.2408	24.8
3.5	17.4	104.6	0.1763	0.3080	35.3
4.0	21.3	96.0	0.2872	0.4281	47.2
4.5	25.1	88.9	0.4189	0.5633	60.6
5.0	28.6	82.9	0.5715	0.7121	75.4
5.5	31.9	77.7	0.7404	0.8732	91.5
6.0	35.0	73.3	0.9249	1.0448	109.0
6.5	38.0	69.3	1.1233	1.2261	127.6
7.0	40.7	65.8	1.3342	1.4164	147.6
7.5	43.3	62.7	1.5565	1.6134	168.6
8.0	46.0	59.9	1.7891	1.8178	191.2
8.5	48.5	57.4	2.0309	2.0281	214.8
9.0	50.8	55.1	2.2811	2.2451	239.5
9.5	53.0	53.0	2.5390	2.4675	265.4
10.0	55.2	51.0	2.8042	2.6961	292.3

* All cross sections are in millibarns (10^{-31} m^2) per orbital iron electron.
** Displacements are for 40 eV threshold.

(Step 7) Total Displacement Cross Section for Gamma Rays

The displacement cross section for a gamma ray undergoing Compton scattering is simply the total Compton cross section times the number of displacements per event. A similar product is made for pair-formation events. These factors, for 40 eV, are included in Table I. The sum of the two products is then the total displacement cross section for iron as a function of gamma-ray energy. The sum for 40 eV is the final column of Table I. Figure 2 graphically displays the total displacement cross section for both thresholds.

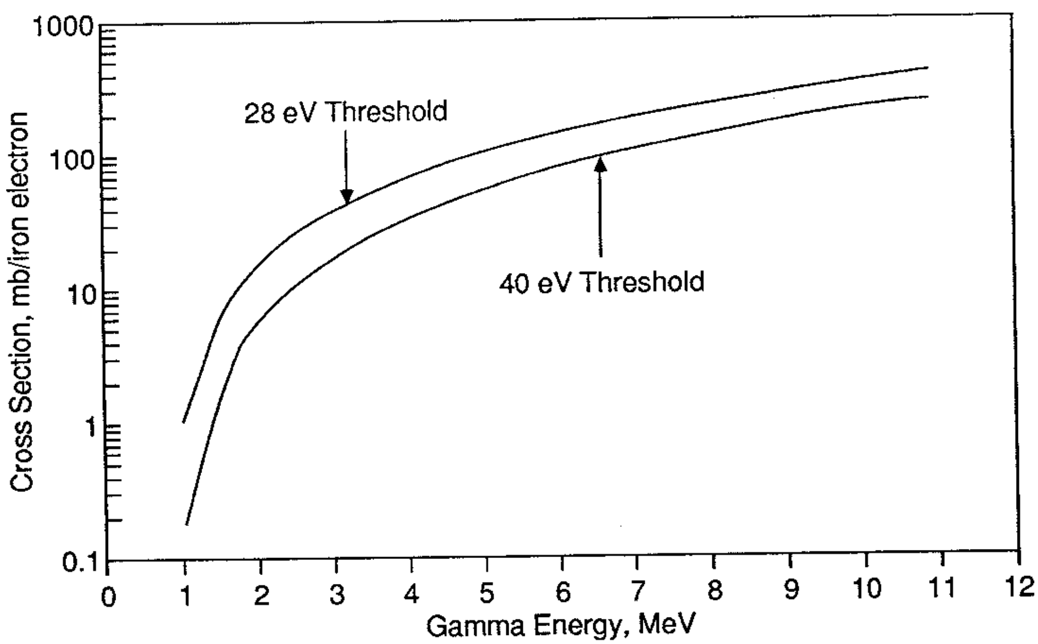

Figure 2. Gamma-Ray Displacement Cross Section in Iron

M91feb032.01
02-21-91

Gamma-Ray Fields in SRS Reactor Tank Walls

A rigorous computation of gamma-ray transport from the core of the reactor to the tank wall requires a code which couples neutrons and gamma rays in an eigenvalue solution. At the present, SRS has no analytic transport code with this capability. The SRS version of ANISN [8] has a coupled 22-group neutron/gamma ray set of cross sections, but performs only "shielding" calculations, which include only first generation fission and capture events. In order to use this code to estimate neutron and gamma-ray transport, the energy and space distribution of the neutron and gamma fluxes in the core must be known a priori. Various SRS codes can calculate the space distribution of the neutron flux fairly accurately. In typical SRS lattices, gamma rays can be assumed to have the same distribution over the core.

For the present study, the lattice selected was a homogenized tritium producing lattice of D_2O, U-235, Li-6, and Al with (or without) a homogenized blanket of D_2O, Li-6, and Al. The blanket, when present, replaces fuel in the outermost ring of lattice sites. The radial distribution of the source was taken to be flat out to, but not including, the last ring of fuel for both blanketed and unblanketed cases with a reduced source strength in the outer ring. With this distribution, the ANISN computed ratio of thermal neutron flux at the tank wall to that in the core (Table II) agreed well with values computed by more sophisticated reactor transport codes (8.2% and 1.97% vs. 7% and 2%). The reference thermal neutron displacement cross section in Table II is that for iron atom recoil following neutron capture and gamma emission.

Table II
Thermal Neutron and Gamma Fluxes in Reactor Tank Wall
(Normalized to thermal neutron flux in core)

Group	No Blanket Normal	No Blanket Poisoned	With Blanket Normal	With Blanket Poisoned	Displ. Xsctn Barns
Thermal Neutrons	.08200	.000952	.01972	.0001112	11.9
Gammas					
6-10 MeV	.02444	.00315	.00638	.00152	3.1
5-6	.00639	.00159	.00188	.00080	2.4
4-5	.00639	.00375	.00239	.00185	1.6
3-4	.00973	.00717	.00387	.00340	1.0
2-3	.02126	.01116	.00721	.00509	.41
0.9-2	.07033	.05626	.02521	.02272	.07
Neutron Disp'ments	.976	.011	.229	.0013	
Gamma Disp'ments	.1245	.0352	.0367	.0176	

In Table II, the two columns labelled "poisoned" were special computational cases used to separate the effect of core gamma rays from that of capture gamma rays originating at or near the tank wall. For these cases, strong Li-6 absorber, with no capture gamma rays, was added in the vicinity of the tank and shield walls. This virtually eliminated neutron capture in the tank and shield walls without significantly affecting the direct gamma transport from the core. The poisoned and unpoisoned cases can then be algebraically manipulated to separate the neutron capture and transport components.

Normalized to displacements from gamma recoil, the contribution for the full-core lattice (unblanketed) is 9.3% from neutron capture in the wall and shield and 3.4% from core transport. The corresponding values for the blanketed lattice are 8.4 % and 7.8% respectively. The contribution from neutron capture in the wall and shield, about 9%, is nearly independent of core configuration. The component for gamma rays transported from the core does show a strong dependence on lattice configuration. The value of 7.8% for the blanketed tritium producer lattice is near maximum for the various historic lattices at SRS. Although the damage from gamma displacements will never be dominant, in portions of the SRS tank walls it can exceed 10% of the total. This is just large enough to be included in damage estimates. A generally conservative, but reasonable, inclusion of gamma ray damage in SRS reactors can be made by simply augmenting the gamma recoil cross section for thermal neutrons by 15%.

ACKNOWLEDGEMENT

The information contained in the document was developed during the course of work under Contract No. DE-AC09-89SR18035 with the U.S. Department of Energy. By acceptance of this paper, the publisher and/or recipient acknowledges the U.S. Government's right to retain a nonexclusive, royalty-free license in and to any copyright covering this paper along with the right to reproduce, and to authorize others to reproduce all or part of the copyrighted document.

REFERENCES

[1] M. T. Robinson, "The Theory of Radiation Induced Defect Production", International Conference on Radiation Damage in Metals, Gatlinburg, TN, (CONF-751006-15), October 1975.

[2] D. G. Doran, "Neutron Displacement Cross Sections for Stainless Steel and Tantalum Based on a Lindhard Model", Nucl. Sci. Eng.,49, pp 130-144, 1972.

[3] R. Gold, J. H. Roberts, and D. G. Doran, "Determination of Gamma-Ray-Induced Displacement Rates", Reactor Dosimetry: Methods, Applications, and Standardization, ASTM STP 1001, Harry Farrar and E. P. Lippincott, eds, American Society for Testing and Materials, Philadelphia, pp 603-613, 1989.

[4] S. M. Seltzer and M. J. Berger, "Evaluation of the Collision Stopping Power of Elements and Compounds for Electrons and Positrons", Int. J. Appl. Radia. Isot. 33, pp 1189-1218, 1982.

[5] O. S. Oen, "Cross Sections for Atomic Displacements in Solids by Fast Electrons", U.S.A.E.C. Report ORNL-4897, 1973.

[6] E. Segre, "Experimental Nuclear Physics", Vol I, pp 317-325, 1953, John Wiley and Sons, Inc, New York.

[7] P. V. C. Hough, "Low Energy Pair Formation", Phys. Rev. 74, 574, 1948.

[8] W. W. Engle, Jr., "A User's Manual for ANISN", ORNL Report K-1693, March 30, 1967.